A Mechanistic Study of a Gas-Phase Ion/Molecule Reaction between $CH_2NH_2^+$ and CH_4

Satoshi OKADA,* Yasuo ABE, Setsuo TANIGUCHI, Shinichi YAMABE,† and Tsutomu MINATO††
Radiation Center of Osaka Prefecture, Shinke-cho, Sakai 593
†Educational Technology Center, Nara University of Education, Takabatake-cho, Nara 630
††Institute for Natural Science, Nara University, 1500 Misasagi-cho, Nara 631
(Received October 31, 1988)

A gas-phase ion/molecule reaction starting from (CH_4^+ and N_2O)/(CH_4 and N_2O^+) is studied using a pulsed-discharge high-pressure mass spectrometer and the ab initio MO calculation. Two dominant ions, $C_2H_6N^+$ and $C_3H_8N^+$, are recognized; they are formed by the methylation of CH_4N^+. The $C_2H_6N^+$ is formed via the following two reactions:

$$CH_2NH_2^+ \text{ (or } CH_3NH^+) + CH_4 \longrightarrow (CH_3)_2NH_2^+ \quad (5)$$

$$(CH_3)_2NH_2^+ \longrightarrow CH_3NHCH_2^+ + H_2 \quad (7)$$

The methylation is composed of the heterolytic CH_3^+-H^- addition to the C=N bond of CH_4N^+ and the subsequent H_2 elimination. The growth of the ion by the methylation is largely exothermic, while the H_2 elimination has a large energy barrier on the potential energy surface.

Methane is an inert molecule and does not react in condensed media. However, in the gas phase, some unique reactions[1-3] are observed. Field[1a] and Ausloos[1c] have investigated the ionic reactions, the photolysis, and the radiolysis of CH_4. In those reports, secondary and higher-order reactions of CH_4 with the reactive species (ions, radicals, etc.) generated by these processes have been found. Moreover, Hiraoka[1f] has reported a slow ion/molecule reaction of $C_2H_5^+$ with CH_4. In CH_4/N_2O, Ryan[2] and McAllister[3] have reported the minor formation of CH_4N^+ at a low pressure. In spite of these gas-phase studies, however, the ion structure of CH_4N^+ and the reaction mechanism for the formation of this ion have not yet been made clear.

In this work, a gas-phase ion/molecule reactions in CH_4/N_2O is studied using pulsed-discharge high-pressure mass spectrometry. The time profiles of ions formed at high pressures are extensively analyzed, and these ion species are identified by using, as a labelled compound, CD_4 instead of CH_4. The purpose of this work is to clarify experimentally and theoretically why such simple and small cations as CH_4^+ and N_2O^+ may give larger cationic products in the ion/molecule reaction of (CH_4^+ and N_2O)/(CH_4 and N_2O^+).

Experimental

Apparatus and Reagents. The measurements were done with a pulsed-discharge high-pressure mass spectrometer. The primary ionization of reactant gases in an ion source of chemical ionization[4] and an atmospheric-pressure-ionization mass spectrometer[5] was performed with a Townsend-discharge ion source. In our experiment, the temperature of the ion source is easily controllable in the absence of such filaments as rhenium and tungsten. Then, in the pulsed-discharge ion source, a usual electron trap of a commercially available mass spectrometer was replaced with a discharge electrode.

Figure 1 shows schematic diagrams of the discharge-ion source and pulse circuit. The pulse-timing sequence generated by this circuit and the pulse-counting diagram are shown in the figure. The discharge ion source consists of a tip with a height of 0.1 mm on the flat surface of a stainless steel (3.5 mmϕ×1.6 mm) as the cathode and an 85% transmission gold-clad tungsten screen as the anode, while the potential is that of the ionization chamber. The distance between the cathode and anode was fixed at about 3 mm. The distance from the center of the discharge point to the ion-exit slits was 9 mm; the ion-exit slits, 2×0.01 mm, were made of two stainless steel razor blades. The potential of the

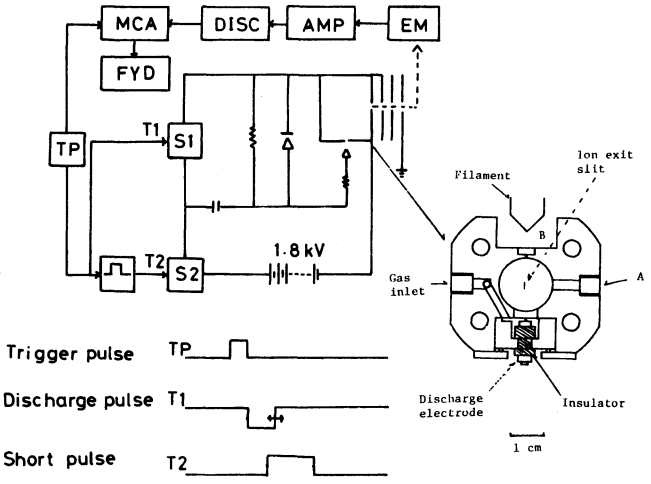

Fig. 1. Schematic diagrams of the discharge ion source and pulse circuit. The pulse timing sequence generated by this pulse circuit and pulse counting diagram are shown. EM: secondary electron multiplier; AMP: amplifier; DISC: discriminator; MCA: multichannel analyzer; FYD: floppy disk drive; TP: trigger pulse; T_1,T_2: discharge and short pulses; S_1,S_2: switching circuits.

first lens with ion-exit slits to prevent field penetration induced by the electric field of the focusing lens was identical with that of the ionization chamber. The pulsed discharge was carried out by two switching circuits (S_1, S_2) using the electric charge and discharge in the capacitor. Since the discharge pulse T_1 tailed for several hundred μs after discharge, the positive pulse T_2 was applied to the discharge electrode to exclude this tailing. In this way, the pulse width of T_1 was decreased to about 30 μs. The discharge-pulse width and the amplitude of T_1 were monitored indirectly with an oscilloscope. Under typical operating conditions, the discharge pulse width, amplitude, and repetition frequency of T_1 were 30 μs, 1.44 kV, and 200 Hz respectively.

The pressures of CH_4 and N_2O in two 10-dm^3 reservoirs were measured with an MKS Baratron model 221 A capacitance manometer. The CH_4/N_2O mixture thus obtained was introduced into the ion source through a Granville–Phillips model-203 manually variable leak. The sample pressure in the ion source was measured with an MKS manometer connected to the gas-inlet line to the ion source. This pressure was corrected with another MKS manometer connected directly to the hole A in Fig. 1 by means of a separate measurement. The correction factor was 0.923. The ion source was heated using an electron-emitting rhenium filament; the maximum temperature obtained was about 453 K. During the present experiments, the holes, A and B, were closed.

In Fig. 1, the time-resolved mass-selected ions formed in the ion source have been accumulated in a multichannel analyzer (Nuclear Data ND 100). Then, the data obtained were transferred to a floppy disk (FYD) and were analyzed with a computer.

The ion-source pressure was in the range from 226.6 to 306.6 Pa, and the flow rate of sample gas was about 0.4 cm^3 s^{-1}. The gases used were methane (Takachiho research grade; 99.95% CH_4), dinitrogen monoxide (Showa Denko, Ltd.; 99.995% N_2O), and methane-d_4 (Merck Sharp and Dohme; 99.5 atom% D). The dinitrogen monoxide was purified by vacuum distillation several times through P_2O_5 chilled with liquid N_2. A trace amount of CO_2 in N_2O was decreased by the use of an Ascarite II trap (20—30 mesh) from Author H. Thomas Co. However, the experimental results obtained were not seriously affected by the Ascarite II. The contents of water and ≧C_2 hydrocarbons in the methane were suppressed by passing the methane through liquid N_2 or Dry Ice–acetone cooled Molecular Sieves. The purities of the methane and dinitrogen monoxide were checked gas-chromatographically using a Pora PLOT Q column of 0.32 mmϕ×10 m at 100 °C. The contents of the ≧C_2 hydrocarbons contained in those samples were less than 1 ppm.

In spite of the general complexity of electrical discharges, the Townsend discharge source[4a] afforded mass spectra that were essentially identical to those obtained with the conventional filament-operated chemical ionization sources. The mass spectra obtained with the Townsend-discharge source have contained only a low abundance of several polymeric reactant ions of a higher mass (m/z>41).

In this study, since the DC discharge was pulsed, it is possible to generate a low current of electricity. Therefore, it seems that the pulsed-discharge ion source suppresses the complexities of the discharge;[6] in fact, the reproducibility of experiments (after six months) could be confirmed.

In the present experiments, the measured total ion current decreased rapidly with a decrease in the temperature of the ion source and the content of CH_4 in the CH_4/N_2O mixture. Headley et al.[7] have reported similar phenomena when oxygen containing molecules such as NO, CO, CO_2, N_2O, and dioxane were used as the reactant gases. Therefore, the experimental conditions are controlled so that the temperature and ratio of the $[CH_4]/[N_2O]$ mixture were kept above 398 K and ≧0.8 respectively. In the text and the **Appendix**,

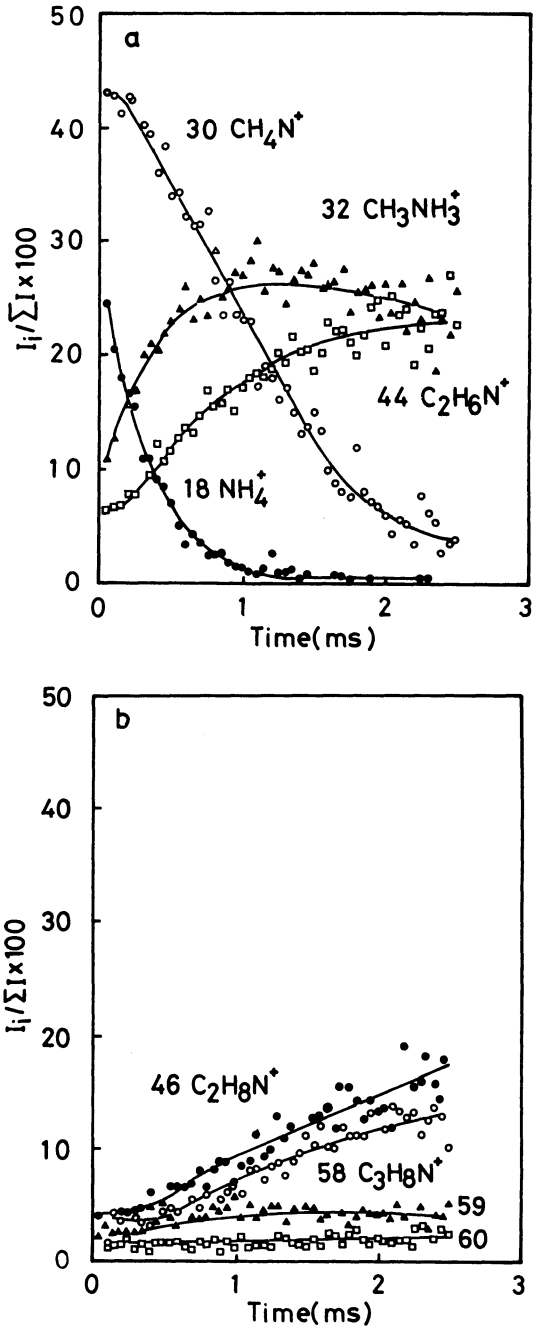

Fig. 2. Normalized ion intensities vs. reaction time observed in CH_4/N_2O mixture at $[CH_4]/[N_2O]$=1.2, T=404 K, P=275.9 Pa. In the figure, mass numbers (m/z) and possible ions are indicated. a is for ions with m/z≦44 and b is for m/z≧46, respectively.

Reactions (1), (2),···(7) are the major ones, while (A), (B),···(H) are side reactions.

Calculations. The ab initio MO calculation was made using the GAUSSIAN 82 program.[8] The 3-21G basis set was used for the geometry optimization. To obtain accurate energies, the single-point calculation on the 3-21G geometry was made with the third-order Møller-Plesset perturbation of the 6-31+G* basis set (MP3/6-31+G*//RHF(or UHF)/3-21G). For the transition state (**TS**) of the H_2 elimination, the vibrational analysis was performed.

Results and Discussion

Experimental. In Figs. 2 and 3, the time profiles of the relative ion intensities of the major ions observed are exhibited. In Fig. 3, CD_4 was used instead of CH_4. The decay curves in Fig. 2 (Fig. 3) are found for *m/z* 18; NH_4^+(ND_4^+(*m/z* 22)), and *m/z* 30; CH_4N^+(CD_4N^+ (*m/z* 34)). The growth curves are observed for *m/z* 32; $CH_3NH_3^+$($CD_3ND_3^+$(*m/z* 38)), *m/z* 44; $C_2H_6N^+$($C_2D_6N^+$ (*m/z* 50)), *m/z* 46; $C_2H_8N^+$ ($C_2D_8N^+$(*m/z* 54)), *m/z* 58; $C_3H_8N^+$, *m/z* 59 and 60. The reaction mechanism of *m/z* 44 and 46 and the results for the minor ions are given in the **Appendix**.

The major cations except the NH_4^+ and the *m/z* 59 ion are found to appear in three groups; (i), (ii), and (iii):

(i) *m/z* 30 CH_4N^+ and *m/z* 32 $CH_3NH_3^+$
(ii) *m/z* 44 $C_2H_6N^+$ and *m/z* 46 $C_2H_8N^+$
(iii) *m/z* 58 $C_3H_8N^+$ and *m/z* 60 $C_3H_{10}N^+$

In each group, the difference in the mass number is 2

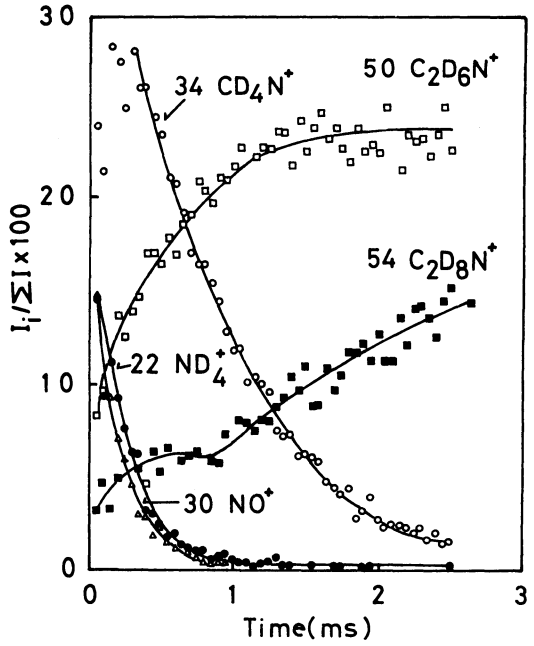

Fig. 3. Normalized ion intensities vs. reaction time observed in CD_4/N_2O mixture at $[CD_4]/[N_2O]$=0.84, *T*=403 K, *P*=295.9 Pa. In the figure, mass numbers (*m/z*) and possible ions are indicated.

(a hydrogen molecule). The growth of the ion size [(i)→(ii)→(iii)] appears to be by the methylation. The decay curve of *m/z* 30, CH_4N^+, indicates that the ion is the precursor for the methylation.

(i) It has been reported[2,3] that the CH_4N^+ was generated from CH_4^+ (*m/z* 16) and N_2O^+ (*m/z* 44) by Reactions (A) and (B). Although the ion intensity for CH_4N^+ has been reported to be very weak under a low pressure (1.3×10^{-1}—1.3×10^{-2} Pa),[3] the large intensity of CH_4N^+ in the present experiments may be due to the large collisional frequency in Reactions (A) and (B), forming intermediate complexes at high pressures (several hundred Pa):

$$CH_4^+ + N_2O \longrightarrow CH_4N^+ + NO \quad (A)$$

$$N_2O^+ + CH_4 \longrightarrow CH_4N^+ + NO \quad (B)$$

As the ion species of *m/z* 60, the association complex$(CH_4\cdot N_2O)^+$ or an intermediate **1** caused by

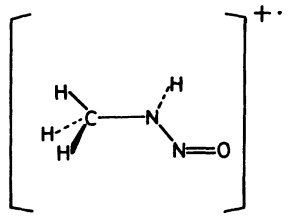

1

the insertion of N_2O into methane is likely. However, the $CD_4\cdot N_2O^+$(*m/z* 64) could not be found under our experimental conditions. Thus, the *m/z* 60 ion assigned to $C_3H_{10}N^+$ in Group (iii), to be described below. Two isomers, $CH_2NH_2^+$ (the methaniminium cation) and CH_3NH^+ (the methylimidogenium cation), appear as the CH_4N^+ (*m/z* 30).[1d,9a] The $CH_2NH_2^+$ is more stable than the CH_3NH^+ (the energy difference in the heat of formation between these ions is 121.2 or 138 kJ mol^{-1}).[10] Moreover, it has been reported[1d] that the first electronically excited state of the $CH_2NH_2^+$ is 2 eV above its ground state. The ionic species of CH_4N^+ forming $C_2H_6N^+$ and $C_2H_8N^+$ by the ion/molecule reactions with CH_4 must be the CH_3NH^+ or the electronically excited state of the $CH_2NH_2^+$.[1d]

The overall disappearance-rate constant of CH_4N^+ for CH_4 was estimated to be ca. 1×10^{-14} cm^3/molecule·s at a temperature of 391—403 K, and concentration of $[CH_4]$, from 5.60 to 13.6×10^{16} molecule/cm^3. A similar slow reaction rate constant has been found[1f] in the ion/molecule reaction of $C_2H_5^+$ with CH_4 to form *s*-$C_3H_7^+$ and H_2 (*k*=ca. 10^{-14} cm^3/molecule·s at 300 K).

The $CH_3NH_3^+$ may be formed by the reaction between NH_4^+ and CH_4, but the ion is not related to the subsequent methylation. This process will be discussed as Reaction (F) in the **Appendix**.

(ii) Several isomers have been reported[9b,c,11] for

the $C_2H_6N^+$ (m/z 44) and $C_2H_8N^+$ (m/z 46). These ions were generated by the ion/molecule reaction of CH_4N^+ with CH_4. The $C_2H_6N^+$ (m/z 44) may be the $CH_3CHNH_2^+$ (ΔH_f=656.8 kJ mol^{-1})[9b] or $CH_3NHCH_2^+$ (ΔH_f=694.5 kJ mol^{-1}).[9b] As the $C_2H_8N^+$ (m/z 46) ion, the $CH_3CH_2NH_3^+$ (ΔH_f=574.8 kJ mol^{-1})[12,13] or $CH_3NH_2CH_3^+$ (ΔH_f=588.6 kJ mol^{-1})[14] is likely from the enthalpy change in the reactions.

The isomerization from $CH_3CHNH_2^+$ to $CH_3NHCH_2^+$ and that from $CH_3CH_2NH_3^+$ to $CH_3NH_2CH_3^+$ have

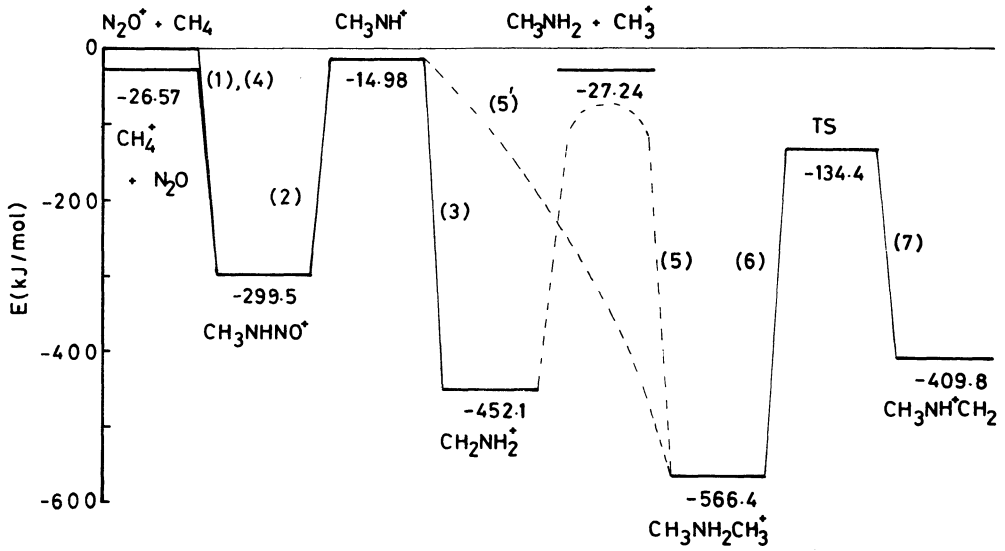

Fig. 4. The energetics of $C_2H_8N_2O^+$ evaluated with the MP3/6-31+G*//HF/3-21G method. The numbers (1)—(7) are defined in charts 1 and 2. The stabilizing energies in kJ mol^{-1} relative to the total energy of (N_2O^++CH_4+CH_4) are shown.

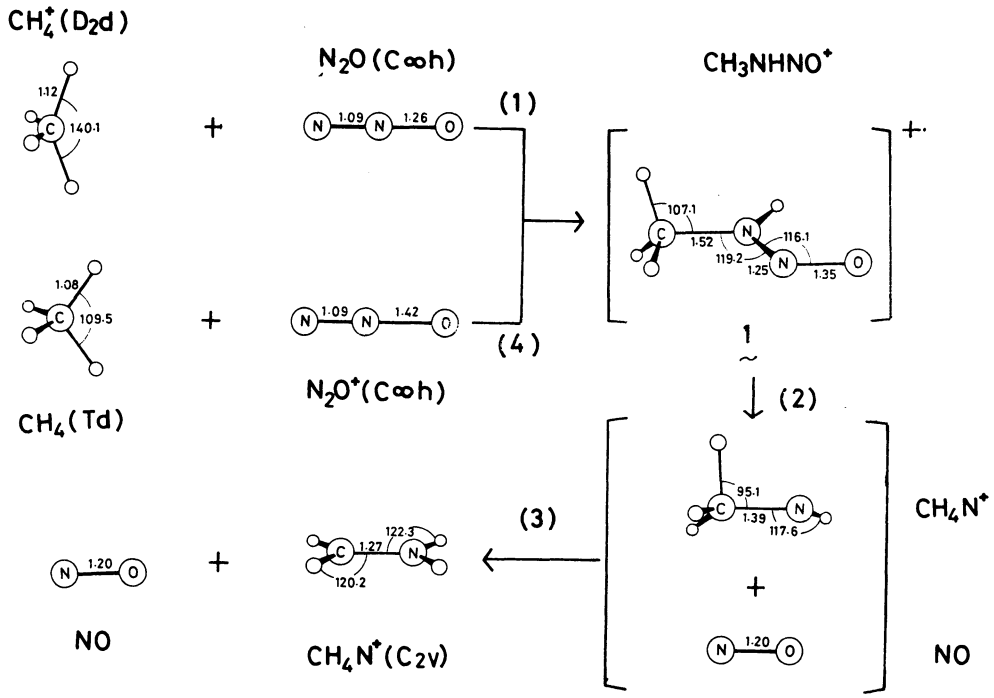

Fig. 5. 3-21G optimized geometries of neutral and cation species involved in reactions (1), (2), (3), and (4). The lengths are in Å and angles in degrees, respectively. The empty circles denote hydrogen atoms.

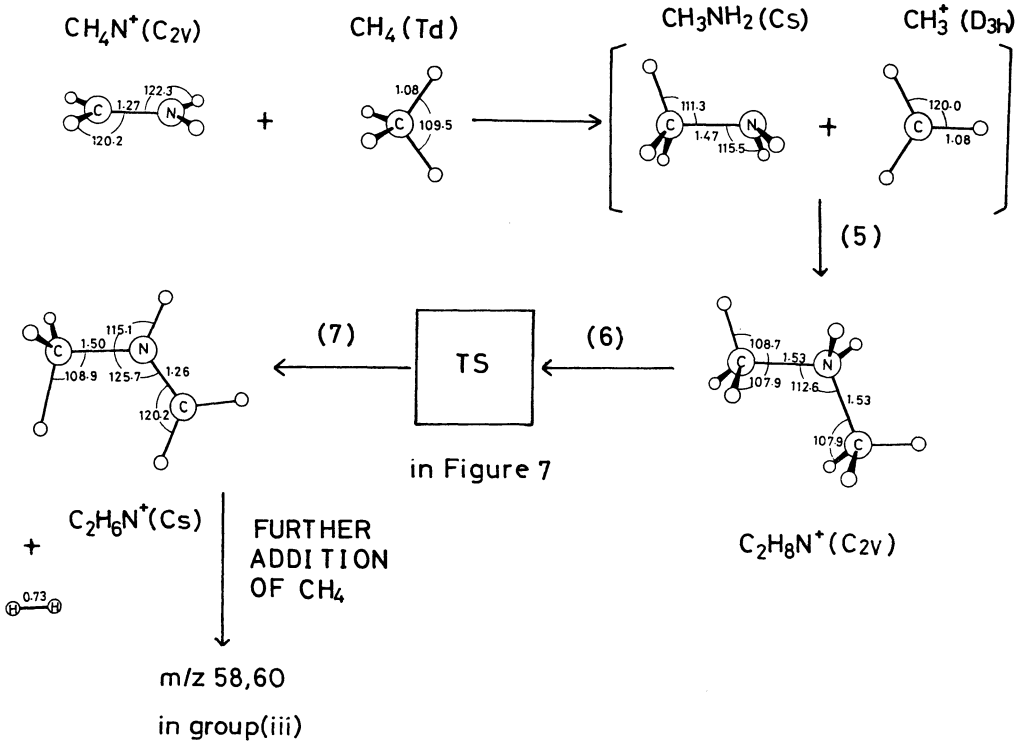

Fig. 6. 3-21G optimized geometries of neutral and cation species involved in reactions (5), (6), and (7).

very high barriers, estimated to be ΔH=ca. 401[11] and >418 kJ mol^{-1}.[15] These isomers, therefore, have been shown to be non-interconvertible under the usual mass-spectrometric conditions.

In the present experiment, the detected ions, m/z 30, 44, and 46, may be identified according to Bowers's result.[15] The m/z 30 ion is $CH_2NH_2^+$, the m/z 46 ion is $CH_3NH_2CH_3^+$ (and partly $CH_3CH_2NH_3^+$), and the m/z 44 ion is $CH_3NHCH_2^+$. The detailed discussion of this assignment will be given at the beginning of the **Appendix**.

(iii) For the $C_3H_8N^+$, several isomers have been reported;[9b] $(CH_3)_2CNH_2^+$ (ΔH_f=589.9 kJ mol^{-1}), $CH_3CHNHCH_3^+$ (ΔH_f=615 kJ mol^{-1}), $CH_3CH_2CHNH_2^+$ (ΔH_f=635.9 kJ mol^{-1}), $CH_3CH_2NHCH_2^+$ (ΔH_f=652.7 kJ mol^{-1}), and $(CH_3)_2NCH_2^+$ (ΔH_f=661 kJ mol^{-1}). Among these ions, the most stable isomer is $(CH_3)_2CNH_2^+$. However, the ion species formed by the ion/molecule reaction of $C_2H_6N^+$ with CH_4 is not clear experimentally. The formation and subsequent reactions of these ions must, therefore, be examined theoretically.

Computational. Of the three groups, the ions of (ii) and (iii) seem to be formed by a similar reaction pattern. Since the molecular size of Group (iii) is large, we will restrict ourselves to the cations in Groups (i) and (ii) for the computational analysis.

In Fig. 4, the energy diagram of Charts 1 and 2 is shown. In Figs. 5—7, the geometries of the reactants

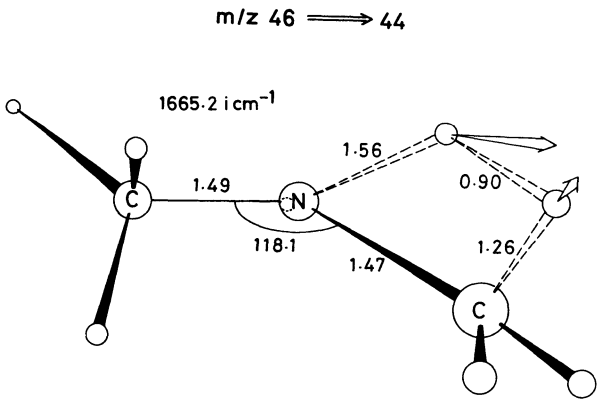

Fig. 7. The transition-state (TS) structure of H_2 elimination in reactions (6) and (7). The reaction coordinate vector corresponding to the sole imaginary frequency 1665.2i cm^{-1} is sketched. Note that a hydrogen atom ((shown by a broken circle)) stays behind the nitrogen atom.

and intermediates are displayed. In Fig. 4, the system of $(CH_4^+ + N_2O)$ is only 26.56 kJ mol^{-1} more stable than that of $(CH_4 + N_2O^+)$. This small energetic difference suggests that both systems are precursors of further reactions. The potential energies vary considerably alnog with the reaction process, which suggests that all the intermediate species are quite "hot" molecules. For instance, the energy level of the transition state of the H_2 elimination is lower than that of the precursor

Chart 1. Possible Reactions (1)—(4) to Generate the CH_4N^+ Species

Reactions	ΔH_r/kJ mol^{-1} Exptl[a]	Calcd[b]
$CH_4^+ + N_2O \xrightarrow{(1)} [1] \xrightarrow{(2)} CH_3\text{-}NH^+ + NO \xrightarrow{(3)} CH_2NH_2^+ + NO$ (m/z 16 → m/z 30)	−397.1 (−413.8)	−425.5
$N_2O^+ + CH_4 \xrightarrow{(4)} [1] \xrightarrow{(2)} CH_3\text{-}NH^+ + NO \xrightarrow{(3)} CH_2NH_2^+ + NO$ (m/z 44 → m/z 30)	−420.2 (−436.9)	−454.8

a) $\Delta H_f(CH_4^+)$=1150 kJ mol^{-1} from Ref. 13a. $\Delta H_f^{298}(CH_2NH_2^+)$=744.7 kJ mol^{-1} from Ref. 9b. $\Delta H_f(N_2O^+)$=1330 kJ mol^{-1} from Ref. 13a. $\Delta H_f^{298}(N_2O)$=82.04 kJ mol^{-1}, $\Delta H_f^{298}(NO)$=90.24 kJ mol^{-1}, and $\Delta H_f^{298}(CH_4)$=−74.80 kJ mol^{-1} from Ref. 13a. The values in parenthesis were estimated using $\Delta H_f^{298}(CH_2NH_2^+)$=728 kJ mol^{-1} from Ref. 9a. b) Computed with the MP3/6-31+G* method.

$CH_4^+ + N_2O$. The sufficient kinetic and vibrational energies accumulated may make the reactions in Charts 1 and 2 likely. In Fig. 4, the energy level of CH_3NH_2 plus CH_3^+ is shown. The level is regarded as the upper boundary of the barrier energy of the hydride-ion shift and the methyl-cation migration. The cooperative mechanism will lower the barrier energy to make Reaction (5) a facile process.

The $(CH_4 \cdot N_2O)^+$ species (m/z 60) **1**, which is ruled out by the experiment using a deuterium compound, is calculated to be stable by 284.5 kJ mol^{-1} relative to CH_3–NH^+ plus NO. Under the present condition (404 K), however, the lifetime of **1** would be too short to be observed in Fig. 2. This is because the hot molecule **1** has enough energy accumulated by insertion to decompose into $CH_4N^+ + NO$.

In Chart 1, four reactions-(1), (2), (3), and (4)- are displayed. Two isomers[1d,9a,d] of CH_4N^+ are considered. One is CH_3–NH^+, while the other is CH_2=NH_2^+. Although a carbene-type form is obtained for CH_3–NH^+, the stability is sensitive to the method of computation.[16] Indeed, the ethylidene CH_3–CH, which is isoelectronic with CH_3–NH^+, has been reported by Pople et al. to be absent.[17] Therefore, CH_3–NH^+ is only a transient species, and CH_2=NH_2^+ (isoelectronic with ethylene) is the sole stable species. In Chart 1, the CH_3NH^+ is shown to be first formed by the insertion of N_2O^+/N_2O into a C–H bond of CH_4/CH_4^+ via **1**. The insertion can be explained by an orbital interaction like the insertion of CH_2 or NH into a C–H bond.[18] For instance, the interaction (in the figure of the frontier orbitals) is effective in the insertion. The charge-transfer (**CT**) interaction from the **HOMO** of the C–H bond to the **SOMO** of N_2O^+ is the driving force of the reaction. In the case of Reaction (1) in Chart 1, the **CT** from the **HOMO** of N_2O to the **SOMO** of CH_4^+ is the driving force. This CH_3–NH^+ isomerizes to CH_2=NH_2^+.

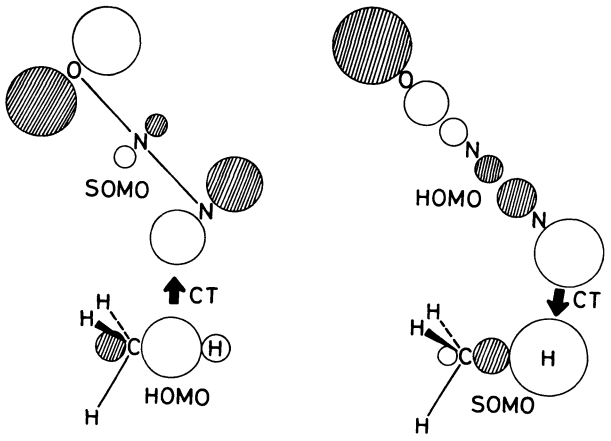

Under the present high pressure (P=275.9 Pa), the transient ion may collide with neutral molecules, H_2 and CH_4, prior to its arrival at CH_2=NH_2^+. If CH_3-NH^+ reacts with H_2, $CH_3NH_3^+$ (m/z 32) in Group (i) may be formed. If CH_3–NH^+ reacts with methane in Chart 2, the protonated dimethylamine (m/z 46) in Group (ii) is produced. The transition-state search for this route was attempted, but we failed to arrive at the energy maximum. Thus, Route (5)′ seems not to include an energy barrier. The reaction of CH_2=NH_2^+ with CH_4 in Route (5) to form the protonated dimethylamine is also likely. The CH_2=NH_2^+ stays at the electronically excited state or at a high vibrational state, as is shown by the large exothermicity in Chart 1. The energy-rich species may cause the hydride-ion shift and the subsequent methyl-cation addition.

The isolation of the methyl cation is unlikely, because the lone-pair electrons on the nitrogen atom capture the cation instantly. Once the $(CH_3)_2NH_2^+$ ion is formed, the dehydrogenation shown in Chart 2 is expected to give m/z 44 in Group (ii). From the protonated dimethylamine, the *N*-methylmethaniminium cation may be produced. The transition state (**TS**)

Chart 2. Addition Reactions to Form $C_2H_6N^+$ and $C_2H_8N^+$ from CH_4N^+

Reactions					ΔH_r/kJ mol^{-1}	
					Exptl[a]	Calcd[b]
m/z 30		*m/z* 46				
$CH_2NH_2^+$	+ CH_4	⟶	$(CH_3)_2NH_2^+$	(5)	−81.3 (−64.6)	−114.2
CH_3-NH^+	+ CH_4	⟶	$(CH_3)_2NH_2^+$	(5)′		
m/z 46						
$(CH_3)_2NH_2^+$		⟶	TS	(6)		
TS		⟶	$CH_3NHCH_2^+$ *m/z* 44	+ H_2 (7)	24.6[c] (41.3)[c]	42.3[c]

a) $\Delta H_f^{298}(CH_2NH_2^+)$=744.7 kJ mol^{-1} from Ref. 9b. $\Delta H_f^{298}(CH_4)$=−74.80 kJ mol^{-1} from Ref. 13a. $\Delta H_f^{298}((CH_3)_2NH_2^+)$=588.6 kJ mol^{-1} from Ref. 14. $\Delta H_f^{298}(CH_3NHCH_2^+)$=694.5 kJ mol^{-1} from Ref. 9b. The values in parenthesis were estimated using $\Delta H_f^{298}(CH_2NH_2^+)$=728 kJ mol^{-1} from Ref. 9a. b) Computed with the MP3/6-31+G* method. c) Experimental and calculated ΔH_r for the formation of $CH_3NHCH_2^+$ is calculated from the reaction, $CH_2NH_2^+ + CH_4 \rightarrow CH_3NHCH_2^+ + H_2$.

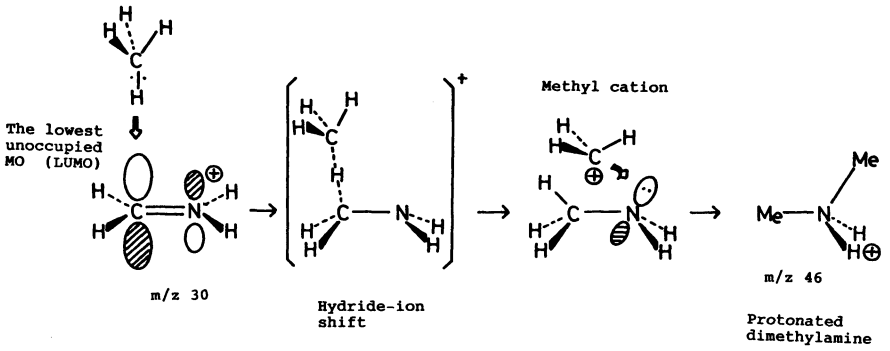

structure of the dehydrogenation is explicitly determined (It is shown in Fig. 7).

In view of the reaction patterns in Chart 2, the formation of Group (iii) may be deduced. To give the *m/z* 60 species, the H_3C-HN^+=CH_2 should be a precursor for two species in Group (iii):

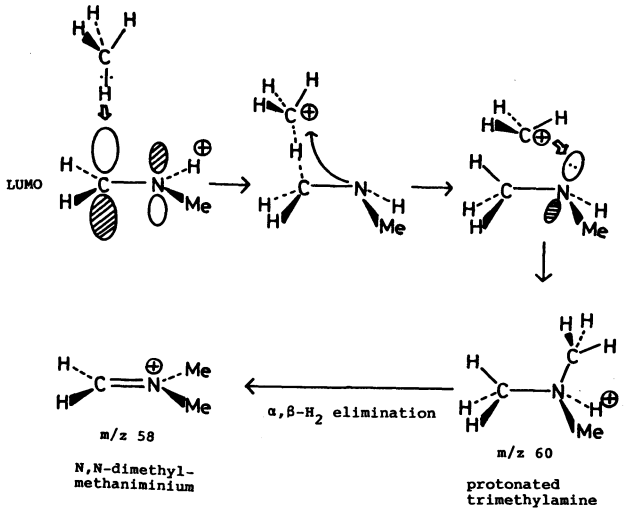

The *m/z* 60 cation is obtained by the methane addition to H_3C-HN^+=CH_2, followed by the H_2 elimination to give *m/z* 58. According to this scheme, the methane addition to CH_2=$N^+(CH_3)_2$ (*m/z* 58) can possibly give CH_3-$N^+(CH_3)_3$ (*m/z* 74), but the formation of *m/z* 72 is unlikely because of the absence of the α,β-H_2 elimination. That is, the *m/z* 74 is the end of the chain reaction of methane addition and H_2 elimination.

Bowers et al.[15] have reported that Reactions (5) and (6) in Chart 2 have the large barriers on the basis of metastable and collision-induced studies of $C_2H_8N^+$. From Fig. 4, the values for these two reactions are estimated to be below 424.9 (−27.24—(−452.2), upper boundary) and 432 (−134.4—(−566.4)) kJ mol^{-1} respectively.

Concluding Remarks

Methane is a rigid, ball-type molecule, and its reaction is improbable in the sense of organic chemistry. However, in the gas phase, specific patterns of chain-type reactions (formally, the methylation) have been observed.[1f,19,20]

The CH_4N^+ ion (*m/z* 30) is the key precursor for the growth of the ion size. The methylation is composed of the heterolytic CH_3^+-H^- addition to the C=N double bond and the subsequent α,β-H_2 elimination. That is, the methane addition is initiated by the hydride ion sharing by two cations. This is followed by the

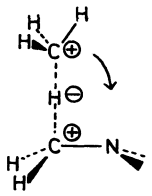

methyl-cation 1, 2 shift toward the nitrogen lone-pair electrons. The H_2 elimination occurs by a combination of the *N*-protonated hydrogen and the methyl hydrogen. The high vibrational state of the C–H stretching will make the elimination a facile process (cf. Fig. 7). The methylation is terminated when a hydrogen atom connected to the nitrogen atom is not available. That is, $N(CH_3)_4^+$ (*m/z* 74) will be the final product, although no species with this large mass number is detected here.

Thus, the growth of the mass number is the substitution process of protonated amines and imines, primary→secondary→tertiary.

As an important result, the activation energy for the H_2 elimination was quantitatively calculated.

Appendix

***m/z* 46 and 44.** The results by collision-induced dissociation[15] have indicated that, for $CH_3CH_2NH_3^+$ (*m/z* 46), only one metastable dissociation reaction (C) was observed and that there is not a significant barrier in the reverse reaction. Also, it has been shown that, for $CH_3NH_2CH_3^+$, the metastable reactions forming $CH_3NHCH_2^+$ (*m/z* 44) and $CH_2NH_2^+$ (*m/z* 30) were observed, while the reverse reactions of Eqs. (D) and (E) have large activation barriers. (The values were not estimated.)

$$\underset{(m/z\ 46)}{CH_3CH_2NH_3^+} \longrightarrow \underset{(m/z\ 18)}{NH_4^+} + C_2H_4 \qquad (C)$$

$$\underset{(m/z\ 46)}{CH_3NH_2CH_3^+} \longrightarrow \underset{(m/z\ 44)}{CH_3NHCH_2^+} + H_2 \qquad (D)$$

$$\underset{(m/z\ 46)}{CH_3NH_2CH_3^+} \longrightarrow \underset{(m/z\ 30)}{CH_2NH_2^+} + CH_4 \qquad (E)$$

In the present experiments, some ions (*m/z* 30, 44, and 46) are detected. Of these, *m/z* 46 and 44 must be formed by the reverse reaction of (E) and the forward reaction (D) respectively, although the details of these reaction mechanism are unknown.

The Minor Ions. *m/z* 18(NH_4^+). The NH_4^+ (*m/z* 18) in Fig. 2 may be yielded by the following two reactions:

i) The proton transfer from the carbonium ions[12] and hydronium ions, etc., to a trace amount of NH_3, whose ions were found by the ion/molecule reactions in CH_4. The NH_3 is contained in the reaction system as an impurity or is generated by the pulsed discharge in the CH_4/N_2O mixture.

ii) The direct routes forming NH_4^+ by means of ion/molecule reactions.

The decrease in the relative ion intensity of NH_4^+ (*m/z* 18) in the range of reaction times of 0—1 ms may be due to Reaction (F), corresponding to the increase in that of $CH_3NH_3^+$ (*m/z* 32):

$$NH_4^+ + CH_4 \xrightarrow{k} CH_3NH_3^+ + H_2 \qquad (F)$$

The overall disappearance-rate constant of $I_{18}/\Sigma I$, *k* (the nomalized ion intensity of NH_4^+, where I_{18} denotes the ion intensity of *m/z* 18), was determined to be $(3\pm0.5)\times10^{-14}$ cm³/molecule·s. This slow rate constant may be due to the endothermicity (ΔH_r=55.22 kJ mol⁻¹) of Reaction (F).

***m/z* 30(NO^+) and *m/z* 46(NO_2^+).** Nitrogen monoxide, NO^+ (*m/z* 30), and NO_2^+ (*m/z* 46) ions are present as other ionic species of *m/z* 30 and 46. However, the results in Fig. 3 show that the relative ion intensity of NO^+ (*m/z* 30) decreased until the reaction time of <0.3 ms. The intensity of NO^+ decreases rapidly, which indicates that the ion reacts with some neutral molecules. A check was made to see whether or not these are higher hydrocarbons as impurities derived in the reagents. In the literature,[9-11] *m/z* and the intensities of the products of reactions between NO^+ and hydrocarbons are available. Fortunately, none of the cited ions were found in our experiment. Thus, the contribution of higher hydrocarbons (as well as ethane) to the reaction with NO^+ may be neglected.

The neutral molecule is expected to be methane, thus giving the following two reactions:

$$NO^+(a^3\Sigma^+) + CH_4 \longrightarrow CH_4^+ + NO \qquad (G)$$

$$NO^+ + CH_4 \longrightarrow \underset{N\text{-hydroxymethaniminium ion}}{CH_2{=}NH(OH)^+} \qquad (H)$$

Eq. (G) is a charge transfer-reaction with a large rate constant (k=ca. 1.0×10^{-9} cm³/molecule·s). Eq. (H) is an insertion with a large exothermicity (ΔH_r=−180.3 kJ mol⁻¹ computed with MP3/6-31+G*//RHF/3-21G). Although the result for NO_2^+ (*m/z* 46) is not shown in the figure, the relative ion intensity of NO_2^+ (*m/z* 46) was very weak (<several%) and independent of the reaction time. Therefore, the contribution of NO^+ and NO_2^+ to the decrease in CH_4N^+ (*m/z* 30) and the formation of $C_2H_8N^+$ (*m/z* 46) could be eliminated by the longer reaction time (>0.3 ms).

***m/z* 59.** The ion species of *m/z* 59 seems to be $C_3H_7O^+$ (oxygen-containing ion)[13] for the following reasons: i) the relative ion intensity of *m/z* 59 increased with the increase in the content of H_2O in the reaction system; ii) in an experiment using CD_4, *m/z* 66 ($C_3D_7O^+$) was detected as the corresponding ion.

Nitrogen-Containing Molecules besides $C_2H_6N^+$ and $C_2H_8N^+$. If trace amounts of the nitrogen-containing molecules—NH_3, CH_3NH_2, C_2H_7N, etc.— are present in the reaction system as impurities or as products of the pulsed discharge, the formation of CH_4N^+ (*m/z* 30),[1d,e,g,25] $CH_3NH_3^+$ (*m/z* 32), and $C_2N_8N^+$ (*m/z* 46)[25-27] may be, in part, due to the contribution of these molecules. Particularly, the growth curve of $C_2D_8N^+$ (*m/z* 54) in Fig. 3 is somewhat complicated. A part of the increase in $C_2D_8N^+$ may be due to the proton transfer to a trace amount of C_2D_7N. However, the reactions for the formation of $C_2H_6N^+$ (*m/z* 44) are unlikely.[25-27] Munson[26] has reported that the rate of hydride transfer is about one-fifth that of proton transfer, judging from the ratio of the increase in the relative ion

intensities of $(CH_3)_2NCH_2^+$ (m/z 58) and $(CH_3)_3NH^+$ (m/z 60) in $(CH_3)_3N$. The ratio of the increase in the relative ion intensity of these ions in Fig. 2 is different from Munson's result. Our data show that the increase in the relative ion intensity of $C_3H_8N^+$ (m/z 58) is larger than that of $C_3H_{10}N^+$ (m/z 60). This suggests that $C_3H_8N^+$ (m/z 58) and $C_3H_{10}N^+$ (m/z 60) in Fig. 2 were formed by the ion/molecule reaction of $C_2H_6N^+$ with CH_4.

The authors wish to thank the Data Processing Center of Kyoto University for the allotment of the CPU time on the FACOM M-380 Computer. Thanks are also due to the Institute for Molecular Science for the use of the HITAC M-680H computer.

References

1) a) F. H. Field, J. L. Franklin, and M. S. B. Munson, *J. Am. Chem. Soc.*, **85**, 3575 (1963). b) F. P. Abramson and J. H. Futrell, *J. Chem. Phys.*, **45**, 1925 (1966). c) R. Gorden, Jr., and P. Ausloos, *J. Chem. Phys.*, **46**, 4823 (1967). d) W. T. Huntress, Jr., and D. D. Elleman, *J. Am. Chem. Soc.*, **92**, 3565 (1970). e) W. T. Huntress, Jr., R. F. Pinzzotto, Jr., and J. B. Landenslager, *J. Am. Chem. Soc.*, **95**, 4107 (1973). f) K. Hiraoka and P. Kebarle, *J. Chem. Phys.*, **63**, 394 (1975). g) G. P. K. Smith, M. Saunders, and R. J. Cross, Jr., *J. Am. Chem. Soc.*, **98**, 1324 (1976).

2) K. R. Ryan and P. W. Harland, *Int. J. Mass Spectrom. Ion Phys.*, **15**, 197 (1974).

3) T. McAllister, *Int. J. Mass Spectrom. Ion Phys.*, **25**, 55 (1977).

4) a) D. F. Hunt, C. N. McEwen, and T. M. Harvey, *Anal. Chem.*, **47**, 1730 (1975). b) D. F. Hunt, G. C. Stafford, Jr., F. W. Crow, and J. W. Russell, *Anal. Chem.*, **48**, 2098 (1976).

5) a) M. M. Shahin, *J. Chem. Phys.*, **45**, 2600 (1965). b) E. C. Horning, M. G. Horning, D. I. Carroll, I. Dzidic, and R. N. Stillwell, *Anal. Chem.*, **45**, 936 (1973). c) H. Kambara and I. Kanomata, *Anal. Chem.*, **49**, 270 (1977). d) I. Dzidic, D. I. Carroll, R. N. Stillwell, and E. C. Horning, *Anal. Chem.*, **48**, 1763 (1976).

6) For example, ethane (C_2H_6), etc., or the nitrogen-containing molecules (NH_3, etc.) would be formed by the discharge.

7) J. V. Headley, R. S. Mason, and K. R. Jennings, *J. Chem. Soc., Faraday Trans. 1*, **78**, 933 (1982).

8) J. S. Binkley, M. J. Frisch, D. J. DeFrees, K. Raghavachari, R. A. Whiteside, H. B. Schlegel, E. M. Fluder, and J. A. Pople, GAUSSIAN 82, Carnegie-Mellon University, Pittsburg, PA 15213 U.S.A.

9) a) J. E. Collin and M. J. Franklin, *Bull. Soc. R. Sci. Liege*, **35**, 267 (1966). b) F. P. Lossing, Y.-T. Lam, and A. Macoll, *Can. J. Chem.*, **59**, 2228 (1981). c) V. Barone, F. Lelj, P. Grande, and N. Russo, *THEOCHEM*, **124**, 319 (1985). d) M. M. Bursey, D. J. Harvan, C. E. Parker, J. A. Darden, and J. R. Hass, *Org. Mass Spectrom.*, **18**, 530 (1983).

10) $\Delta H_f^{298}(CH_2NH_2^+)$=728 and 744.7 kJ mol^{-1} were used from Refs. 9a and 9b. $\Delta H_f^{298}(CH_3NH^+)$=866 kJ mol^{-1} is taken from Ref. 9a.

11) R. D. Bowen, D. H. Williams, and G. Hvistendahr, *J. Am. Chem. Soc.*, **99**, 7509 (1977).

12) $\Delta H_f^{298}(CH_3CH_2NH_3^+)$=574.8 kJ mol^{-1} is calculated by using $\Delta H_f^{298}(CH_3CH_2NH_2)$=−47.15 kJ mol^{-1} from Ref. 13a. $PA(CH_3CH_2NH_2)$=907.9 kJ mol^{-1} and $\Delta H_f^{298}(H^+)$=1530 kJ mol^{-1} are from Ref. 13b.

13) a) *J. Phys. Chem. Ref. Data*, **6**, I-776, I-777 (1977). b) *J. Phys. Chem. Ref. Data*, **13**, 703, 709 (1984).

14) $\Delta H_f^{298}((CH_3)_2NH_2^+)$=588.6 kJ mol^{-1} is calculated by using $\Delta H_f^{298}((CH_3)_2NH)$=−18.45 kJ mol^{-1} from Ref. 13a. $PA((CH_3)_2NH)$=922.9 kJ mol^{-1} and $\Delta H_f^{298}(H^+)$=1530 kJ mol^{-1} are from Ref. 13b.

15) M. F. Jarrold, N. J. Kirchner, S. Liu, and M. T. Bowers, *J. Phys. Chem.*, **90**, 78 (1986).

16) A theoretical calculation of the H_2 elimination, $CH_4N^+ \longrightarrow CH_2N^+ + H_2$, with the 6-31G** basis set has been reported recently: K. F. Donchi, B. A. Rumpf, G. D. Willett, J. R. Christie, and P. J. Derrick, *J. Am. Chem. Soc.*, **110**, 347 (1988). The instability of the CH_3–NH^+ species has been pointed out there.

17) K. Raghavachari, M. J. Frisch, J. A. Pople, and P. von R. Schleyer, *Chem. Phys. Lett.*, **85**, 145 (1982).

18) M. S. Gordon and D. R. Gano, *J. Am. Chem. Soc.*, **106**, 5421 (1984).

19) F. H. Field and M. S. B. Munson, *J. Am. Chem. Soc.*, **87**, 3289 (1965).

20) M. Meot-Ner, *Origins of Life*, **9**, 115 (1978).

21) K. Hiraoka, K. Aoyama, and K. Morise, *Can. J. Chem.*, **63**, 2899 (1985).

22) "Gas-Phase Ion-Molecule Reaction Rate Constants Through 1986," ed by Y. Ikezoe, S. Matsuoka, M. Takebe, and A. Viggiano, Maruzen Press, Tokyo (1987).

23) D. F. Hunt and T. M. Harvey, *Anal. Chem.*, **47**, 2136 (1975).

24) R. Chal and A. G. Harrison, *Anal. Chem.*, **55**, 969 (1983).

25) E. G. Jones and A. G. Harrison, *Can. J. Chem.*, **45**, 3119 (1967).

26) M. S. B. Munson, *J. Phys. Chem.*, **70**, 2034 (1966).

27) J. M. Brupbacher, C. J. Eagle, and E. Tschuikow-Roux, *J. Phys. Chem.*, **79**, 671 (1975).